# Elastic/Crystalline Viscoplastic Finite Element Analysis of the Deep Drawing Process, Taking Account of Texture Structure

*by Hideo Morimoto* and Eiji Nakamachi *2*

**ABSTRACT** Earing is a phenomenon that is characteristic of deep drawing, the most commonly used method for the press forming of thin sheet, and is caused by the anisotropy of the material. This gives importance to techniques for controlling the texture structure by taking account of this anisotropy to. In this way the properties of the material are used to best advantage and adverse effects are reduced. The means increasingly used to accomplish this is finite element analysis.

In the present work, the authors have developed a method of elastic/crystalline viscoplastic finite element analysis which directly applies crystalline plasticity theory to the deep drawing of aluminum alloys.

Models were constructed, and different crystal orientations were introduced to investigate the relationship between deformation and texture structure, yielding appropriate analytical results that agreed with inferences based on tensile tests of the materials.

## 1. INTRODUCTION

Deep drawing is the commonest method of press forming thin sheets, and plays an important role in 3-dimensional forming of sheet stock. Products that depend on deep drawing are met with in many fields, from automobile bodies to home appliances and kitchen utensils.

The most characteristic phenomena that attend deep drawing are wrinkling and earing. Earing is an unevenness at the upper edge of the product, and is caused by anisotropy produced by biased crystal orientation, that is to say by the texture structure, during rolling of the material. Earing is categorized in terms of type and degree into 45° earing (a total of four protrusions occurring at an angle of 45° with respect to the rolling direction of the material) and 0/90° earing (a total of four protrusions occurring in the rolling direction or at an angle of 90° thereto).

In recent years progress has been made in developing crystal control techniques that result in sheets having superior formability to suppress earing and necking. The authors have accordingly developed a method of finite element analysis using a mathematical model based on crystal structure, and have applied it to actual drawing conditions.[1),2)]

Conventionally in finite element analysis, anisotropy has been modeled as changes in a yield surface, and various proposals have been made, most conspicuously Hill's yield function,[3)] but these have mainly been useful when load history was comparatively simple and the parameters of anisotropy did not vary greatly. There are thought to be many difficulties in the way of developing a yield surface model that takes account of the deformation-dependence of anisotropy.

In investigating the effect of texture structure on deep drawing, the present work, therefore, abandons the indirect approach of determining the yield function, and instead adopts a method in which crystalline plasticity theory is applied directly to plastic working analysis. A number of crystal orientations are then introduced into the analytical model to achieve an elastic/crystalline viscoplastic finite element analysis.

## 2. ELASTIC/CRYSTALLINE VISCOPLASTIC CONSTITUTIVE EQUATIONS

In a slip system (a), let $\boldsymbol{m}^{a}$ be the unit vector normal to a slip plane defined by a crystal, and $\boldsymbol{s}^{a}$ be the unit vector in the direction of slip.

These vectors rotate with deformation. Thus if $\boldsymbol{m}^{*a}$ and $\boldsymbol{s}^{*a}$ be the vectors after deformation, we may represent the velocity gradient tensor $\boldsymbol{L}$, the rate of deformation tensor $\boldsymbol{d}$ and the material spin tensor $\boldsymbol{w}$ by the equations

* Materials Research Center, Yokohama Lab., R&D Div.
*2 Materials Strength Lab., Mechanical Engineering Dept., Osaka Institute of Technology

$$\boldsymbol{L} = \boldsymbol{d} + \boldsymbol{w} \quad \cdots\cdots (1)$$

$$\boldsymbol{d} = \boldsymbol{d}^{*} + \boldsymbol{d}^{p}, \quad \boldsymbol{w} = \boldsymbol{w}^{*} + \boldsymbol{w}^{p} \quad \cdots\cdots (2)$$

$$\boldsymbol{L}^{p} = \boldsymbol{d}^{p} + \boldsymbol{w}^{p} = \sum_{a} \dot{\gamma}^{a} \boldsymbol{s}^{*a} \boldsymbol{m}^{*a} \quad \cdots\cdots (3)$$

where the superscript "*" indicates the stretch and spin components, the superscript "p" the slip component, and $\dot{\gamma}^{a}$ the shear strain rate of slip system (a).

The rate deformation tensor plastic portion $\boldsymbol{d}^{p}$ and the spin tensor plastic portion $\boldsymbol{w}^{p}$ are shown by

$$\boldsymbol{d}^{p} = \sum_{a} \boldsymbol{P}^{a} \dot{\gamma}^{a}, \quad \boldsymbol{w}^{p} = \sum_{a} \boldsymbol{W}^{a} \dot{\gamma}^{a} \quad \cdots\cdots (4)$$

where

$$2\boldsymbol{P}^{a} = \boldsymbol{s}^{*a} \boldsymbol{m}^{*a} + \boldsymbol{m}^{*a} \boldsymbol{s}^{*a}, \quad 2\boldsymbol{W}^{a} = \boldsymbol{s}^{*a} \boldsymbol{m}^{*a} - \boldsymbol{m}^{*a} \boldsymbol{s}^{*a} \quad \cdots\cdots (5)$$

If the elastic constitutive equation is unaffected by the slip deformation of the crystal, the rate type constitutive equation will be

$$\hat{\boldsymbol{S}}^{*} = \boldsymbol{D}^{e} : \boldsymbol{d}^{*} \quad \cdots\cdots (6)$$

where $\hat{\boldsymbol{S}}^{*}$ is the objective co-rotational rate of Kirchhoff stress.

A rate type constitutive equation adopting a Jaumann rate $\hat{\boldsymbol{S}}$ obtained using material spin tensor $\boldsymbol{w}$ may be found by

$$\hat{\boldsymbol{S}} = \hat{\boldsymbol{S}}^{*} - \sum_{a=1}^{N} \beta^{a} \dot{\gamma}^{a} = \boldsymbol{D}^{e} : \boldsymbol{d}^{*} - \sum_{a=1}^{N} \boldsymbol{R}^{a} \dot{\gamma}^{a} \quad \cdots\cdots (7)$$

where $\boldsymbol{N}$ is the number of slip systems and $\boldsymbol{R}^{a}$ is as shown in the equation

$$\boldsymbol{R}^{a} = \boldsymbol{D}^{e} : \boldsymbol{P}^{a} + \beta^{a}, \quad \beta^{a} = \boldsymbol{W}^{a} \cdot \sigma - \sigma \cdot \boldsymbol{W}^{a} \quad \cdots\cdots (8)$$

The time derivative of Cauchy stress $\dot{\sigma}$ may then be expressed by

$$\dot{\sigma} = \hat{\boldsymbol{S}} - \sigma \,\mathrm{tr}\, \boldsymbol{L} + \boldsymbol{w} \cdot \sigma - \sigma \cdot \boldsymbol{w} \quad \cdots\cdots (9)$$

In a strain rate dependent crystal slip model, the shear strain rate in crystal slip system (a) $\dot{\gamma}^{a}$ will be determined by Schmid's resolved shear stress $\tau^{a}$ on the slip plane, as shown in the equation

$$\tau^{a} = \boldsymbol{s}^{*a} \cdot \sigma \cdot \boldsymbol{m}^{*a} = \boldsymbol{P}^{a} : \sigma \quad \cdots\cdots (10)$$

and by a parameter determined by the change in the internal structure of the current deformation condition.

As a constitutive equation for shear strain rate $\gamma^{a}$, we adopted the exponential viscoplastic constitutive equations of Hutchinson[4] and Pan-Rice.[5]

$$\dot{\gamma}^{a} = \dot{a}^{a} \left[\frac{\tau^{a}}{g^{a}}\right] \left|\frac{\tau^{a}}{g^{a}}\right|^{\frac{1}{m}-1} \quad \cdots\cdots (11)$$

where $\tau^{a}$ is the resolved shear stress, $g^{a}$ the reference shear stress and $\dot{a}^{a}$ the reference shear strain rate of slip system (a), and $m$ is a strain rate sensitivity exponent. Given that, when shear strain is zero, $g^{a}$ equals the critical resolved shear stress $\tau_0$, we may, with respect to $g^{a}$, use the hardening evolution equation

$$\dot{g}^{a} = \sum_{b=1}^{N} h_{ab} \left|\dot{\gamma}^{b}\right| \quad \cdots\cdots (12)$$

Here $h_{ab}$ is a function of $\gamma$, and we adopt the equations

$$h_{ab} = h(\gamma)\, q_{ab} \quad \cdots\cdots (13)$$

$$h(\gamma) = h_0 n C \{C(\gamma_0 + \gamma)\}^{n-1} \quad \cdots\cdots (14)$$

where $h_0$ is the initial hardening ratio, $C$ the hardening coefficient, $n$ the hardening exponent and $\gamma_0$ the initial shear strain. Further, $q_{ab}$ is a parameter representing the magnitude of self and latent hardening, and is represented by the equation

$$q_{ab} = \begin{bmatrix} C & L_1 & L_2 & L_3 \\ L_1 & C & L_3 & L_2 \\ L_2 & L_3 & C & L_1 \\ L_3 & L_2 & L_1 & C \end{bmatrix} \quad \cdots\cdots (15)$$

where:

$$C = \begin{bmatrix} 1 & q_c & q_c \\ q_c & 1 & q_c \\ q_c & q_c & 1 \end{bmatrix}, \quad L_1 = \begin{bmatrix} q_v & q_l & q_l \\ q_l & q_c & q_l \\ q_l & q_l & q_v \end{bmatrix}$$

$$L_2 = \begin{bmatrix} q_c & q_l & q_l \\ q_l & q_v & q_l \\ q_l & q_l & q_c \end{bmatrix}, \quad L_3 = \begin{bmatrix} q_v & q_l & q_l \\ q_l & q_v & q_l \\ q_l & q_l & q_c \end{bmatrix}$$

and $q_c$ represents the case in which two slip systems are within the same plane or in the same direction, $q_v$ when they are at right angles, and $q_l$ represents other cases. For aluminum alloy, the values of $q_c$, $q_v$ and $q_l$ are 1.0, 1.2 and 1.3.[6]

## 3. ELASTIC/CRYSTALLINE VISCOPLASTIC FINITE ELEMENT ANALYSIS

An elastic/crystalline viscoplastic model was constructed using the shear strain rate-dependent constitutive equation and the n-power hardening evolution equation given in (11) and (12). At the integration point of the 8-node isoparametric 3-dimensional element, a "direct-crystal"

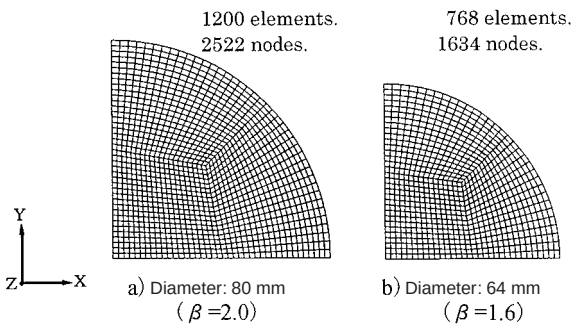


**Figure 1 Analytical models**

model[7] was adopted to allocate crystal orientations.

In the present work, the results of analysis of crystal orientation distribution and tensile tests for pure aluminum were compared with the results of finite element analysis of uni-axial tension to establish parameters and determine the properties of the material.

### 3.1 Materials Model

One method of analyzing problems of plastic working involving anisotropy is to find the yield function by materials testing and then conduct the analysis on the basis of the theory of plasticity for a continuum. If, however, anisotropy is introduced directly in the form of a crystal orientation distribution, the analysis will automatically take into account the development of anisotropy due to deformation. In the present work, analysis was carried out by introducing a number of crystal orientation distributions into a material model described as follows.

Taking account of the drawing ratios suitable for cup deep drawing (β=1.6-2.0), we chose two types of specimens: 1) aluminum sheet 1 mm thick and 80 mm in diameter (β=2.0) and 2) aluminum sheet 1 mm thick and 64 mm in diameter (β=1.6). In consideration of symmetry with respect to the rolling direction, we used the quarter portion of these aluminum sheets. Figure 1 shows the material models used in the analysis.

Elements were divided so that their effective lengths were virtually identical, with a single division in the thickness direction, giving a total of 1200 elements in model 1 and 768 in model 2, and a total number of nodes of 2522 and 1634 respectively. In both models the rolling direction was the y-axis and the thickness direction the z-axis. Planes parallel to the x-axis were confined in the y-axis direction, and planes parallel to the y-axis were confined in the x-axis direction.

The various material parameters used in the analysis were identified using the results of tensile tests using pure aluminum (1050-O) as described above, and are as shown in Table 1.

**Table 1 Material Parameters**

| | | |
|---|---|---|
| Material | | 1050-O |
| Young's modulus | $E$ / GPa | 70.3 |
| Density | ρ / MPa·(mm·s$^{-1}$)$^{-2}$ | 2.7×10$^{-7}$ |
| Anisotropic parameters | $c_{11}$ / GPa<br>$c_{22}$ / GPa<br>$c_{44}$ / GPa | 98.882<br>60.662<br>28.224 |
| Poisson's ratio | ν | 0.345 |
| Friction coefficient | μ | 0.1 |
| Initial reference shear stress | $\tau_0$ / MPa | 10.0 |
| Initial hardening ratio | $h_0$ / MPa | 37.0 |
| Reference shear strain rate | $\dot{a}$ / s$^{-1}$ | 0.01 |
| Strain rate sensitivity exponent | $m$ | 0.07 |
| Work hardening exponent | $n$ | 0.33 |

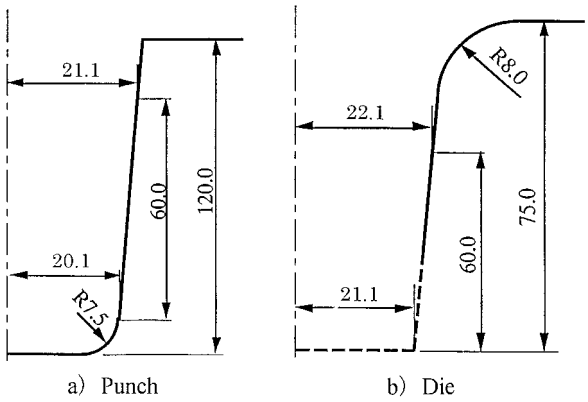


**Figure 2 Tool data**

### 3.2 Tools

It was assumed that the tools used for deep drawing were the cup punch and die shown in Figure 2.

### 3.3 Analytical Conditions

Analyses were carried out using punch speeds of 2 m/s in the case of Model 1 (β=2.0) and 0.5 m/s for Model 2 (β=1.6). To determine the influence of the texture structure of the material, analyses were carried out based on the following three:

a) Cube type (single-crystal, (100)[001] orientation);
b) Brass type (single-crystal, (110)[1$\bar{1}$2] orientation); and
c) Copper type (single-crystal, (121)[1$\bar{1}$1] orientation).

{111} pole figures for each of these texture structures are shown in Figure 5.

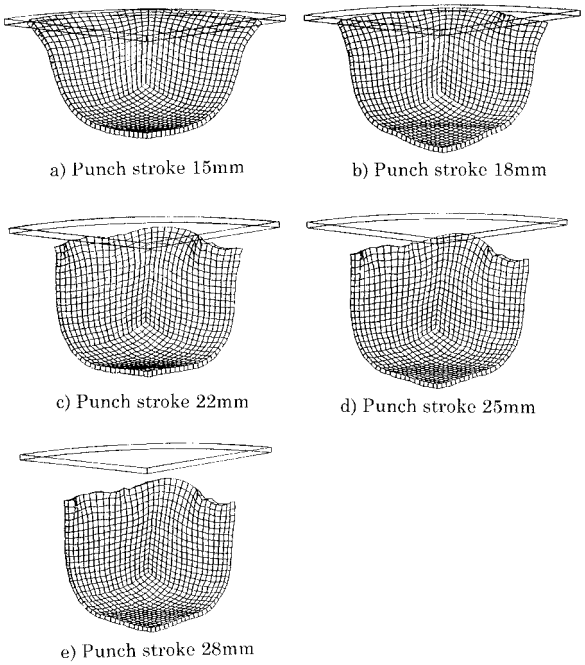


**Figure 3 Deformed shape of brass type structure (β=1.6); outline presents blank before deformation**

## 4. ANALYTICAL RESULTS AND DISCUSSION

### 4.1 Occurrence of Earing and Thickness Strain Distribution

Figure 3 shows the results of analysis of the deformed shape of material during the deep drawing process for material of brass type texture structure with a drawing ratio b of 1.6, and Figure 4 shows the results for thickness strain distribution for cube type texture structure (β=2.0). Figure 5 shows the results of analyses of the thickness strain distribution at a punch stroke of approximately 30 mm (β=2.0) and of the deformed shape at a punch stroke of approximately 28 mm (β=1.6), together with {111} pole figures of each of the three texture structures. The crystal orientation distribution used in analysis is as shown in Figure 5.

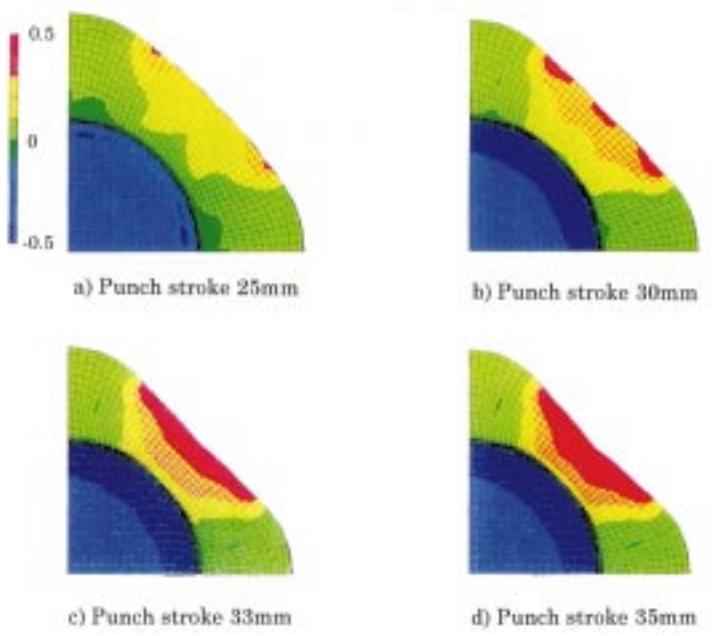


**Figure 4 Thickness strain distribution in cube type structure (cube type, β=2.0)**

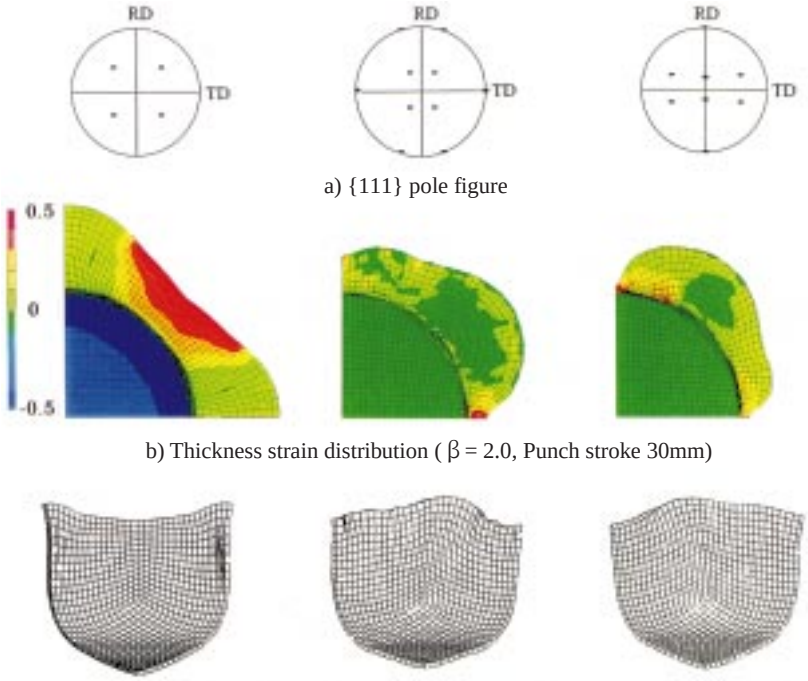


**Figure 5 Thickness strain distribution and deformed shape**

In addition, to illustrate clearly the difference in earing (deformation at the periphery of the test piece after deep drawing), Figure 6 shows the flange edge deformation when β=2.0 at a punch stroke of 27 mm, with the angle from the rolling direction on the horizontal axis and the flange radius in that direction on the vertical axis. Similarly, Figure 7 shows edge deformation when β=1.6 (no flange was formed since test piece diameter was small) at a punch stroke of 28 mm.

From Figures 6 and 7 we can see that for cube-type texture structure, deformation is greatest for material at about 45° from the rolling direction and is drawn into the die cavity, whereas in the 0° and 90° directions, the material tends not to be drawn into the die cavity. In contrast for brass and copper type texture structures, the material is best drawn into the die cavity at angles near 0° and 90°. This shows that there are major differences in deformation depending on the texture structure of the material.

### 4.2 Comparison of Deformation of Deep Drawn Products with Results of Material Tensile Tests

To investigate the relationship between the analytical results described above and the mechanical properties of the materials, 5052-O and 5182-O aluminum alloys were subjected to uni-axial tensile tests and the relationship between stress and strain was found. The tests were conducted using JIS #5 tensile test pieces at a tensile rate virtually identical to the strain rate during ordinary deep drawing.

The materials for the test pieces used in the uni-axial tensile tests were 5052-300, 5052-12 and 5182-12 (where the figures following the hyphens indicate average grain size in μm). The decision to use these materials was based on the results of measurements of the pole figures that are described below.

Figure 8 shows {111} pole figures measured for the three types of aluminum alloys. Observation of the pole figures shows that 5052-12 is a brass-type alloy and 5182-12 is close to copper-type. As for 5052-300, grain size was so large (300 μm) that there was no orientation distribution sufficient to discern the preferred orientation. Based, however, on a report[8] that a cube-type texture structure appeared when annealed (recrystallized) after medium-reduction cold rolling, and on the fact that the effect of heat treatment is greatly magnified when grain size is large, it was concluded that the 5052-300 structure was close to cube-type.

Thus although the materials differed, it is considered appropriate from the standpoint of texture structure, to treat the three alloys 5052-300, 5052-12 and 5182-12 as, respectively, a cube-type, brass-type and copper-type structure.

Figure 9 shows the relationship between true stress and

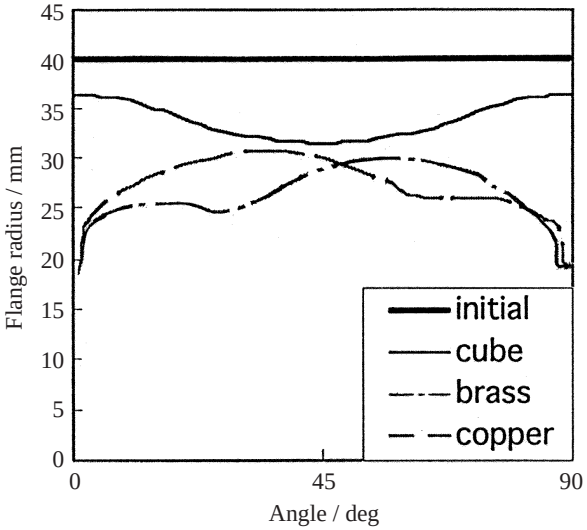


**Figure 6 Relationship between flange radius and angle from rolling direction (β=2.0,punch stroke 27 mm)**

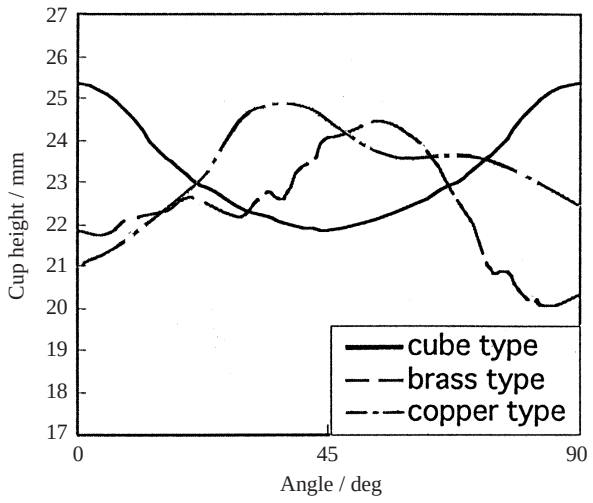


**Figure 7 Relationship between wall height and angle from rolling direction (B=1.6, punch stroke 28 mm)**

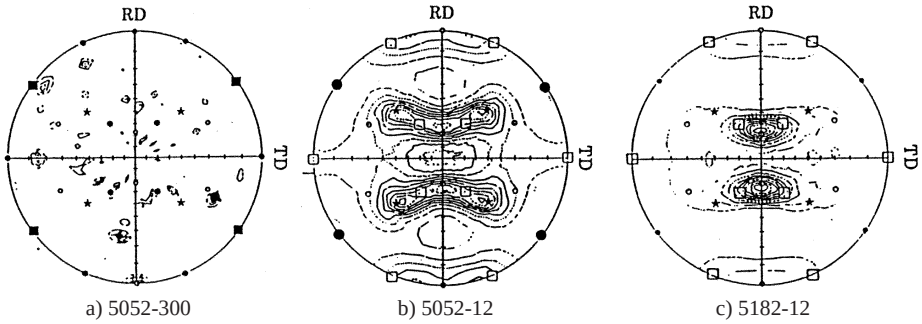


a) 5052-300 b) 5052-12 c) 5182-12

**Figure 8 {111} pole figure**

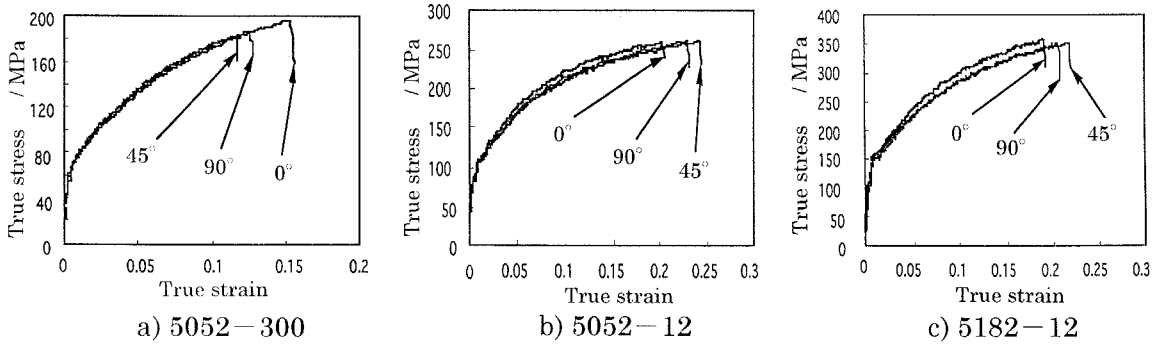


**Figure 9 Relationship between true stress and true strain**

true strain found by uni-axial tensile tests for three types of aluminum alloy sheets, in each of which the tension direction was parallel to, at right angles to and at a 45° angle to the rolling direction. Looking at the stress-strain relationship, fracture strain was smallest in 5052-300 (close to cube-type) test pieces of 45° direction, and strength was high. In the 5052-12 (close to brass-type) and 5182-12 (close to copper-type) test pieces, on the other hand, fracture strain was high in those of 45° direction, and strength was higher in those of direction parallel to and at right angles to the rolling direction.

From these tensile tests results, the following inferences may be made regarding the deformation behavior of products made by cup deep drawing. In the 5032-300 (cube-type) test pieces, strength is higher for the 45° direction and work piece elongation will not take place in that direction, and although the work is drawn into the die cavity, it will be readily elongated in the rolling direction (0°) and in the direction at right angles thereto (90°). It is therefore inferred that earing will occur in the 0° and 90° directions, that is to say 0/90° earing will form. Conversely in the 5052-12 (brass-type) and 5182-12 (copper-type), strength in the 0° and 90° directions is higher than in the 45° direction, so that in those directions the work will be drawn into the die cavity, elongation will be greater in the 45° direction, and 45° earing will form.

The fact that the hypothetical values obtained from tensile tests on the material agree with the analytical results described above suggests that the analytical results obtained in this work are suitable.

## 5. CONCLUSION

The authors have developed a method of elastic/crystalline viscoplastic finite element analysis which adopts crystalline plasticity theory to define the evolution of anisotropy based on the elementary process of crystal slip, instead of conventional plastic potential theory, and applied it to the deep drawing of aluminum alloys.

The influence of the texture structure of the material on deformation of deep drawn products was investigated and the following results were obtained:

(1) Assuming three types of texture structure--cube, brass and copper--analysis was conducted of the cup deep drawing process, revealing a tendency toward 0/90°earing in the cube-type and 45°earing in the brass- and copper-types.

(2) The results of the analysis agreed with those estimated from tensile tests of the materials, suggesting the suitability of the analytical results.

It is planned to apply this analytical method in developing high-formability aluminum alloys.

### REFERENCES

1) H.Morimoto and E.Nakamachi; Proc. 48th Joint Conf. of the Japan Soc. for Technology of Plasticity, (1997), 79. (in Japanese)
2) H.Morimoto and E.Nakamachi; Proc.1998 Spring Joint Conf. of the Japan Soc. for Technology of Plasticity, (1998), 241. (in Japanese)
3) R.Hill; Mathematical Theory of Plasticity, Oxford Press, (1950), 332.
4) J.W.Hutchinson; Proc. R. Soc. London, Ser.A, 384(1975), 101.
5) J.Pan and J.R.Rice; Int. J. Slolids Struct. 19-11(1983), 973.
6) Y.Zhou, K.W.Neal and L.S.Toth; Int. J. Plasticity, 9(1993), 961.
7) E.Nakamchi and X.Dong; Engineering Computations 13-2/3/4(1996),327.
8) K.Itoh; J. of Japan Inst. of Light Metals, 43-5(1993), 285. (in Japanese)

Manuscript received on December 2, 1998.